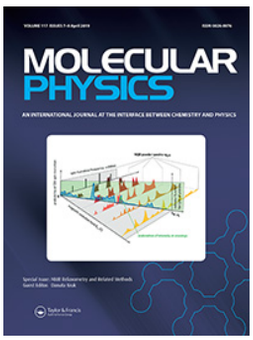

Taylor & Francis
Taylor & Francis Group

Molecular Physics

An International Journal at the Interface Between Chemistry and Physics

ISSN: 0026-8976 (Print) 1362-3028 (Online) Journal homepage: https://www.tandfonline.com/loi/tmph20

^{1}H relaxation and dynamics of triphenylbismuth in deuterated solvents

Danuta Kruk, Elzbieta Masiewicz, Evrim Umut & Hermann Scharfetter

To cite this article: Danuta Kruk, Elzbieta Masiewicz, Evrim Umut & Hermann Scharfetter (2019) ^{1}H relaxation and dynamics of triphenylbismuth in deuterated solvents, Molecular Physics, 117:7-8, 921-926, DOI: 10.1080/00268976.2018.1513175

To link to this article: https://doi.org/10.1080/00268976.2018.1513175

Published online: 29 Aug 2018.

MOLECULAR PHYSICS
2019, VOL. 117, NOS. 7–8, 921–926
https://doi.org/10.1080/00268976.2018.1513175

Taylor & Francis
Taylor & Francis Group

OPEN ACCESS Check for updates

^{1}H relaxation and dynamics of triphenylbismuth in deuterated solvents

Danuta Kruk [a], Elzbieta Masiewicz[a], Evrim Umut[a] and Hermann Scharfetter[b]

[a]Faculty of Mathematics and Computer Science, University of Warmia and Mazury in Olsztyn, Olsztyn, Poland; [b]Institute of Medical Engineering, Graz University of Technology, Graz, Austria

ABSTRACT

^{1}H spin–lattice relaxation experiments have been performed for triphenylbismuth dissolved in fully deuterated glycerol and tetrahydrofuran. The experiments have been carried out in a broad frequency range, from 10 kHz to 40 MHz, versus temperature. The data have been analysed in terms of a relaxation model including two relaxation pathways: ^{1}H-^{1}H dipole–dipole interactions between intrinsic protons of triphenylbismuth molecule and ^{1}H-^{2}H dipole–dipole interactions between the solvent and solute molecules. As a result of the analysis, rotational correlation times of triphenylbismuth molecules in the solutions and relative translational diffusion coefficient between the solvent and solute molecules have been determined. Moreover, the role of the intramolecular ^{1}H-^{1}H relaxation contribution has been revealed, depending on the motional parameters, as a result of decomposing the overall relaxation dispersion profile into contributions associated with the ^{1}H-^{1}H and ^{1}H-^{2}H relaxation pathways. The possibility of accessing the contribution of the relaxation of the intrinsic protons is important from the perspective of exploiting Quadrupole Relaxation Enhancement effects as possible contrast mechanisms for Magnetic Resonance Imaging.

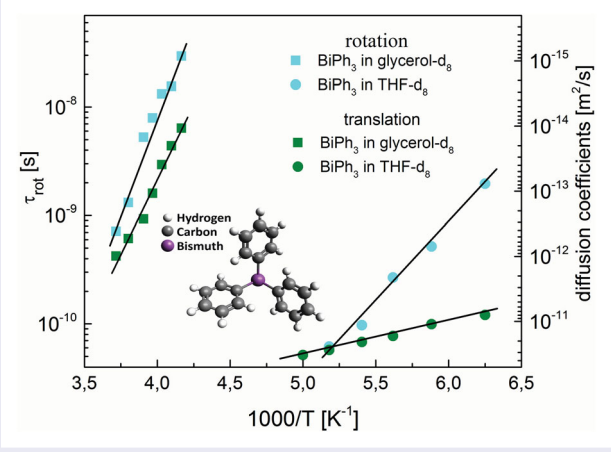

ARTICLE HISTORY
Received 27 June 2018
Accepted 6 August 2018

KEYWORDS
NMR; relaxation; dynamics; contrast

Introduction

Dynamics of binary systems (solutions) raises attention from the viewpoint of fundamental studies and applications. The fundamental question concerning the dynamics of binary systems is about the mutual influence of the components on their motion.

This question can be answered by applying nuclear magnetic resonance (NMR) relaxometry that is a highly appreciated method of studying dynamical processes in condensed matter. The great advantages of NMR relaxometry are its potential to reveal not only the timescale of the dynamical processes, but also their mechanisms, and the ability to probe dynamics of many different timescales in a single experiment [1,2]. This is possible due to the broad range of magnetic fields covered in NMR relaxometry experiments: from 10 kHz to 40 MHz (referring to ^{1}H resonance frequency), while 'classical' relaxation experiments are performed at a single (high) resonance frequency. Nevertheless, despite the advantages of NMR relaxometry, it might be difficult to

CONTACT Danuta Kruk danuta.kruk@matman.uwm.edu.pl Faculty of Mathematics and Computer Science, University of Warmia and Mazury in Olsztyn, Słoneczna 54, Olsztyn 10-710, Poland

unambiguously attribute the observed dynamical processes to the components of the system when the dynamics is on a similar timescale. The way to solve this problem is to deuterate one of the components.

In this work, the procedure has been applied to gain information about the dynamics of triphenylbismuth dissolved in glycerol and tetrahydrofuran. To get direct access to the dynamics of the solute molecules by ^{1}H spin–lattice NMR relaxometry studies the solvents have been deuterated.

The dynamical properties themselves are, however, not the only reason for performing the relaxation studies. Triphenylbismuth includes ^{209}Bi – nucleus of spin $S = 9/2$, possessing a large quadrupole moment. ^{209}Bi containing compounds can potentially be used as novel contrast agents for magnetic resonance imaging (MRI) based on quadrupole relaxation enhancement (QRE) [2–13]. QRE is a complex, quantum-mechanical phenomenon. In the simplest case, it involves one spin $I = 1/2$ (^{1}H) and one spin $S \geq 1$ (for instance ^{209}Bi). The spins are mutually coupled by a magnetic dipole–dipole interaction which is the origin of the I spin relaxation. The energy level structure of the S spin is a result of a superposition of its quadrupole and Zeeman interactions. As the quadrupole interaction is independent of the magnetic field at some magnetic fields the Zeeman splitting of spin I can match one of the transition frequencies of spin S between its energy levels. At these magnetic fields the I spin magnetisation can be transferred to (taken over) by the S spin that manifests itself as an enhancement of the spin–lattice relaxation rate. This effect is frequency specific in contrary to the paramagnetic relaxation enhancement (PRE) [14–18]. The PRE effect is exploited in MRI as a contrast mechanism – it leads to an enhancement of ^{1}H relaxation due to strong proton spin – electron spin dipole–dipole interactions. The effect is modulated by zero field splitting interactions and electron spin relaxation. Although QRE cannot compete with PRE as far as the amplitude of the enhancement is concerned, the high sensitivity of the QRE effect to subtle changes in the electric field gradient caused by even a slight 'molecular rearrangement' in pathological tissues makes the QRE mechanism an interesting alternative to paramagnetic contrast agents. There are several factors that determine the efficiency of QRE as the contrast mechanism. One has to note that the relaxation enhancement concerns the solvent (water) protons. The solvent molecules approach the quadrupole nucleus (^{209}Bi in this case) staying for a while attached to the ^{209}Bi containing species (for instance a nanoparticle containing a ^{209}Bi compound) and then due to exchange dynamics drift to the bulk being replaced by another molecule. The exchange lifetime is a crucial factor as it cannot be neither too short (in such a case the QRE effect will be not 'sensed' by the solvent protons) nor too long (the effect has to be transferred to the bulk during the ^{1}H spin–lattice relaxation process). In this context, it is important to reveal the relaxation features of the intrinsic protons of the ^{209}Bi compound as their relaxation can obscure the QRE effect between the quadrupole nucleus and the solvent protons. Triphenylbismuth is a very promising candidate for QRE based contrast agents due to its large quadrupole coupling leading to relaxation enhancement around the magnetic field of 3T typically used in medical scanners [19–22]. As a continuation of these studies in this paper, we investigate the relaxation and dynamical properties of this compound depending on the viscosity of the solvent.

Theory

The dominating source of ^{1}H relaxation is magnetic dipole–dipole interaction. For proton containing compounds dissolved in deuterated solvents, there are three relaxation pathways: inramolecular and intermolecular ^{1}H-^{1}H dipole–dipole couplings between protons belonging to the solute molecules and intermolecular ^{1}H-^{2}H dipole–dipole coupling between the solvent and solute molecules. The corresponding contributions to the overall relaxation rate, $R_1(\omega_H)$, (ω_H denotes ^{1}H resonance frequency), denoted as $R_{1,\mathrm{intra}}(\omega_H)$, $R^{HH}_{1,\mathrm{inter}}(\omega_H)$ and $R^{HD}_{1,\mathrm{inter}}(\omega_H)$, respectively, are given as [10,16,23–31]:

$$R_1(\omega_H) = R_{1,\mathrm{intra}}(\omega_H) + R^{HH}_{1,\mathrm{inter}}(\omega_H) + R^{HD}_{1,\mathrm{inter}}(\omega_H) \tag{1}$$

where

$$R_{1,\mathrm{intra}}(\omega_H) = C_{DD}[J_{\mathrm{intra}}(\omega_H) + 4J_{\mathrm{intra}}(2\omega_H)] \tag{2}$$

$$R^{HH}_{1,\mathrm{inter}}(\omega_H) = \frac{3}{2}N_H\left(\frac{\mu_0}{4\pi}\gamma_H^2\hbar\right)^2[J_{\mathrm{inter}}(\omega_H) + 4J_{\mathrm{inter}}(2\omega_H)] \tag{3}$$

$$R^{HD}_{1,\mathrm{inter}}(\omega_H) = \frac{4}{3}N_D\left(\frac{\mu_0}{4\pi}\gamma_H\gamma_D\hbar\right)^2[J_{\mathrm{inter}}(\omega_H - \omega_D) + 3J_{\mathrm{inter}}(\omega_H) + 6J_{\mathrm{inter}}(\omega_H + \omega_D)] \tag{4}$$

The dipolar relaxation constant, C_{DD}, in Equation (2) is defined as: $C_{DD} = 3/10(\mu_0/4\pi(\gamma_H^2\hbar/r^3))^2$, where r denotes an effective inter-spin distance.

As the intramolecular dipole–dipole interactions are modulated by rotational dynamics of the molecule, the intramolecular spectra density, $J_{intra}(\omega)$, takes the following form assuming isotropic rotational dynamics of the

solute molecule [24,26,28,29,31]:

$$J_{\text{intra}}(\omega) = \frac{\tau_{rot}}{1+\omega^2\tau_{rot}^2} \tag{5}$$

where τ_{rot} denotes rotational correlation time of the solute molecule, while C_{DD} in Equation (1) is referred to as relaxation dipolar constant. The intermolecular dipole–dipole couplings are primarily modulated by translation diffusion. Assuming the force-free model of translation diffusion the intermolecular spectral density is given as [29,32–35]:

$$J_{\text{inter}}(\omega) = \frac{72}{5}\frac{1}{d^3}\int_0^\infty \frac{u^2}{81+9u^2-2u^4+u^6} \times \frac{u^2\tau_{\text{trans}}}{u^4+(\omega\tau_{\text{trans}})^2}du \tag{6}$$

The translational correlation time, τ_{trans}, is defined as: $\tau_{\text{trans}} = d^2/D_{12}$, where D_{12} denotes a relative translation diffusion coefficient defined as a sum of the diffusion coefficients of the participating molecules, d is referred to as the distance of closest approach for the interacting molecules. This implies that the $R^{HH}_{1,\text{inter}}(\omega_H)$ relaxation contribution depends on the diffusion coefficient of the solute molecules, D^{solute} ($D^{\text{solute}}_{12} = 2D^{\text{solute}}$) and the distance of closest approach, d_{solute}. The parameter N_H is the number of ^{1}H nuclei per unit volume in the solution. Analogously, for the $R^{HD}_{1,\text{inter}}(\omega_H)$ contribution, the parameters are: $D^{\text{solute-solvent}} = D^{\text{solute}} + D^{\text{solvent}}$, $d_{\text{solute-solvent}}$, while N_D is the number of ^{2}H nuclei per unit volume in the solution. The symbols γ_H and γ_D denote gyromagnetic factors of ^{1}H and ^{2}H nuclei, respectively, ω_D is the resonance frequency of ^{2}H.

Experimental details

^{1}H spin–lattice relaxation measurements have been performed for $BiPh_3$ solutions in deuterated glycerol (glycerol-d_8) and deuterated tetrahydrofuran (THF-d_8) in the frequency range of 10 kHz–40 MHz and temperature range of 230–269 K for the first solution and 160–193 K for the second one, using Stelar Spinmaster FFC relaxometer. For the measurements below 10 MHz, the sample has been pre-polarised at a field of 0.57T (corresponding to the frequency of 25 MHz). The number of acquisitions has been set to 8 and 4 for $BiPh_3$ in glycerol-d_8 and $BiPh_3$ in THF-d_8, respectively. Moreover, due to weak dispersion (frequency dependence) of the ^{1}H spin–lattice relaxation for $BiPh_3$ in THF-d_8 the frequency range has been extended to 80 MHz, using 3T magnet compatible with the relaxometer. The concentrations of the solutions are 90 and 80 mM for $BiPh_3$ in glycerol-d_8 and $BiPh_3$ in THF-d_8, respectively. The solution of $BiPh_3$ in glycerol-d_8 has been prepared by dispersing 10 mg of $BiPh_3$ powder in 0.25 ml of glycerol-d_8 and sonicating the mixture for 1 h at 50°C, while

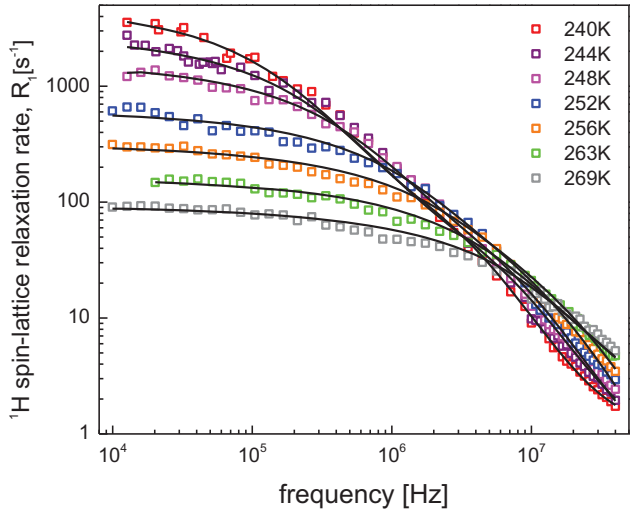

Figure 1. ^{1}H spin–lattice relaxation data for $BiPh_3$ dissolved in glycerol-d_8 (90 mM concentration). Solid lines: theoretical fits.

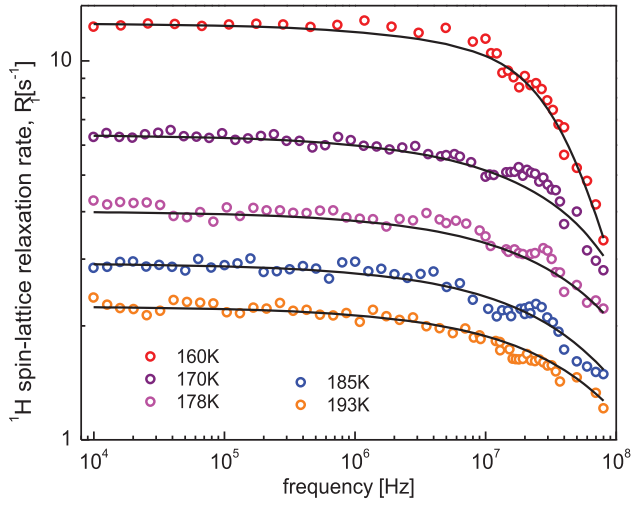

Figure 2. ^{1}H spin–lattice relaxation data for $BiPh_3$ dissolved in THF-d_8 (80 mM concentration). Solid lines: theoretical fits.

Table 1. Parameters obtained from the analysis of ^{1}H spin–lattice relaxation rate profiles for $BiPh_3$ in glycerol-d_8: $N_D = 6.6 \times 10^{-2}$ Å^{-3}, $C_{DD} = 5.25 \times 10^8$ Hz^2

T[K]	τ_{rot}[s]	D[m^2/s]	d[Å]	Relative error [%]
240	2.95×10^{-8}	1.08×10^{-14}	2.73	8.9
244	1.55×10^{-8}	2.01×10^{-14}	2.76	13.8
248	1.32×10^{-8}	3.93×10^{-14}	2.72	15.1
252	7.93×10^{-9}	1.08×10^{-13}	2.72	19.8
256	5.27×10^{-9}	2.68×10^{-13}	2.78	13.6
263	1.31×10^{-9}	5.35×10^{-13}	2.76	9.8
269	7.14×10^{-10}	9.89×10^{-13}	2.78	13.5

Table 2. Parameters obtained from the analysis of ^{1}H spin–lattice relaxation rate profiles for $BiPh_3$ in THF-d_8; $N_D = 5.9 \times 10^{-2}$ Å^{-3}, $C_{DD} = 5.25 \times 10^8$ Hz^2.

T[K]	τ_{rot}[s]	D[m^2/s]	d[Å]	Relative error [%]
160	1.96×10^{-9}	7.95×10^{-12}	2.80	7.5
170	5.18×10^{-10}	1.10×10^{-11}	2.80	14.1
178	2.68×10^{-10}	1.68×10^{-11}	2.79	8.9
185	7.20×10^{-11}	2.07×10^{-11}	2.80	16.1
193	5.36×10^{-11}	2.75×10^{-11}	2.79	17.3
200	1.05×10^{-11}	3.28×10^{-11}	2.84	14.3

the solution of $BiPh_3$ in THF-d_8 has been prepared by dissolving 35 mg of $BiPh_3$ in 1 ml of THF-d_8 without sonication. The chemicals were purchased from Sigma-Aldrich. The deuteration level for glycerol-d_8 and THF-d_8 was 99%.

One should note that there is a different pool of protons in the phenyl rings of $BiPh_3$. The measured ^{1}H spin–lattice relaxation rates represent a mean value for all protons in the molecule.

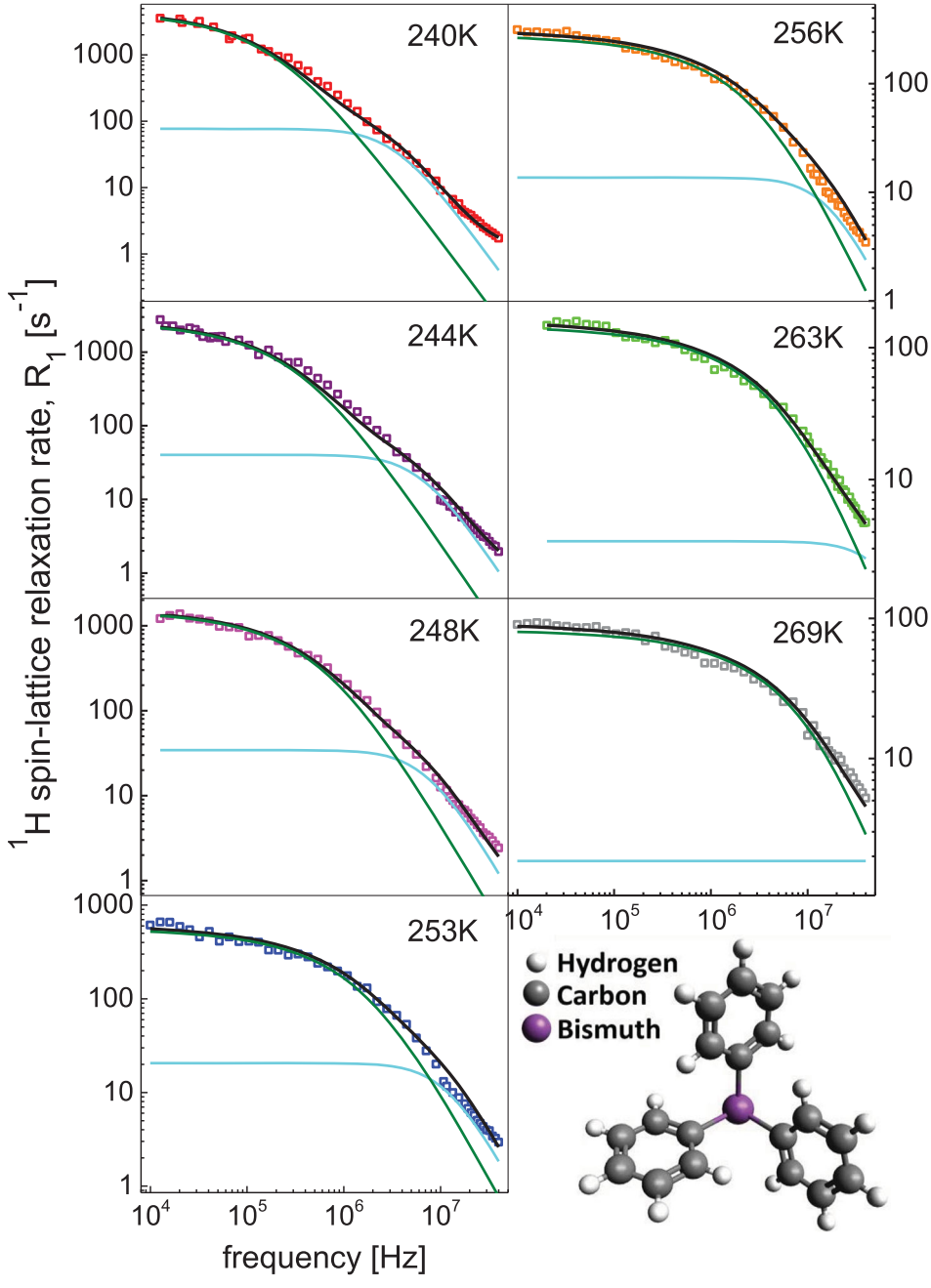

Figure 3. Decomposition of the overall ^{1}H spin–lattice relaxation data for $BiPh_3$ in glycerol-d_8 into the $R_{1,intra}$ (light blue lines) and $R^{HD}_{1,inter}$ (green lines) contributions. The structure of $BiPh_3$ is shown.

Results and analysis

The overall relaxation rate depends on six parameters: C_{DD}, τ_{rot}, D^{solute}, D^{solvent}, d_{solute} and $d_{\text{solute-solvent}}$. It is expected that the diffusion coefficient for the solvent molecules in the solutions is close to those for bulk (pure solvent). Before beginning a quantitative analysis of the relaxation data it is worth to estimate the expected roles of the $R^{HH}_{1,\text{inter}}$ and $R^{HD}_{1,\text{inter}}$ contributions. The key factors that determine the contributions are the gyromagnetic factors, γ_H and γ_D, and the numbers of ^{1}H and ^{2}H nuclei per unit volume: $N_H = 8.1 \times 10^{-4}$ Å^{-3} and $N_D = 6.6 \times 10^{-2}$ Å^{-3} for $BiPh_3$ in glycerol-d_8 and $N_H = 7.2 \times 10^{-4}$ Å^{-3} and $N_D = 5.9 \times 10^{-2}$ Å^{-3} for $BiPh_3$ in THF-d_8. Assuming that the distances of closest approach, d_{solute} and $d_{\text{solute-solvent}}$, are similar and the diffusion coefficients of the solvent and solute molecules do not differ much, the expected ratio $R^{HH}_{1,\text{inter}}/R^{HD}_{1,\text{inter}}$ can be approximated by $(N_H\gamma_H^2/N_D\gamma_D^2) \times 3/8$ (the factor 3/8 stems from the scaling of the relaxation rate with the spin quantum number: $I(I+1)$) that yields about 0.2 for both solutions. In consequence, it seems that the $R^{HD}_{1,\text{inter}}$ contribution to the overall relaxation dominates the $R^{HH}_{1,\text{inter}}$ contribution. To reduce the number of parameters we have decided to neglect the last one. This implies that the experimental data can be fitted in terms of four parameters: C_{DD}, τ_{rot}, $D^{\text{solute-solvent}} = D$ and $d_{\text{solute-solvent}} = d$. The C_{DD} value has been kept the same for both solutions. Figure 1 shows the ^{1}H spin–lattice relaxation data for $BiPh_3$ in glycerol-d_8, while in Figure 2 analogous data for $BiPh_3$ in THF-d_8 are presented. The obtained parameters are collected in Tables 1 and 2 for the glycerol-d_8 and THF-d_8 solutions, respectively. To see the importance of the intramolecular ^{1}H-^{1}H relaxation contribution, in Figure 3 the overall relaxation for the glycerol-d_8 solution has been decomposed into the $R_{1,\text{intra}}$ and $R^{HD}_{1,\text{inter}}$ contributions. The intermolecular ^{1}H-^{2}H contribution dominates at lower frequencies, moreover with increasing temperature fast rotational dynamics diminishes the role of the $R_{1,\text{intra}}$ term.

In Figure 4 the rotational correlation times, τ_{rot}, of $BiPh_3$ in glycerol-d_8 and THF-d_8 have been plotted versus reciprocal temperature. In addition, the values for $BiPh_3$ in glycerol-d_8 have been compared with rotational correlation times obtained for non-deuterated glycerol in bulk [34]. It is interesting to note that the rotational dynamics of $BiPh_3$ in glycerol-d_8 is faster than rotational motion of non-deuterated glycerol molecules in bulk. The activation energies are similar – the lines formed by the solid and open light blue squares are, in good approximation, parallel. One also sees (Figure 4) that the relative translational dynamics of $BiPh_3$ and glycerol-d_8 molecules is faster than for non-deuterated glycerol

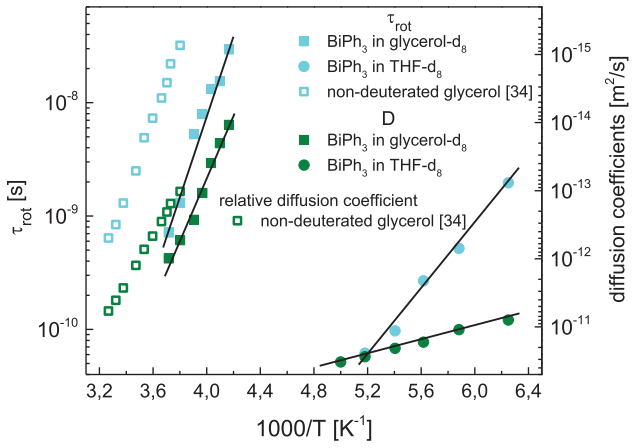

Figure 4. Rotational correlation times τ_{rot} (light blue symbols) for $BiPh_3$ molecules in glycerol-d_8 and THF-d_8 compared with τ_{rot} for glycerol (non-deuterated) in bulk [34]. Solid lines – linear fits according to the Arrhenius law; activation energies: 69.2 kJ/(mol × K) and 27.3 kJ/(mol × K) for the solutions of $BiPh_3$ in glycerol-d_8 and THF-d_8, respectively. Translational diffusion coefficients D between the solvent and solute molecules (green symbols) for $BiPh_3$ in glycerol-d_8 and THF-d_8. For comparison, relative diffusion coefficients for glycerol (non-deuterated) in bulk [34] are shown. Solid lines: linear fits according to the Arrhenius law; activation energies: 86.9 kJ/(mol × K) and 9.5 kJ/(mol × K) for the solutions of $BiPh_3$ in glycerol-d_8 and THF-d_8, respectively.

in bulk. In this case, the activation energies are also similar.

Eventually, it is worth to mention that the contribution to the overall relaxation caused by ^{1}H-^{1}H dipole–dipole interactions between protons of $BiPh_3$ and protons of the non-deuterated fraction of the solvents (the deuteration level is 99%) is of the order of $0.3^*R^{HH}_{1,inter}(\omega_H)$, and therefore one could neglect it.

Conclusions

^{1}H spin–lattice relaxation experiments have been performed for $BiPh_3$ dissolved in glycerol-d_8 and THF-d_8. By using deuterated solvents it has been possible to reveal the relaxation properties of protons of $BiPh_3$ molecules in solution and rotational dynamics of the molecules. It has turned out that the rotational motion of $BiPh_3$ molecules in glycerol-d_8 is faster than the tumbling of non-deuterated glycerol molecules in bulk. Such a comparison can be hardly performed for THF as in this case the rotational motion is very fast rending a weak relaxation dispersion. A similar observation has been made for the relative translational diffusion of $BiPh_3$ and glycerol-d_8 molecules – the diffusion is faster than for non-deuterated glycerol in bulk. In both cases (for the rotational as well as the translational dynamics) the

activation energies are close to those for non-deuterated glycerol in bulk.

The possibility to reveal the role of the $R_{1,\mathrm{intra}}$ relaxation pathway (i.e. the relaxation of intrinsic protons of a ^{209}Bi containing molecule) is important from the perspective of exploiting QRE effects as a contrast mechanism for MRI. The contribution should be negligible compared to the relaxation provided by ^{1}H-^{1}H dipole–dipole interactions between solvent (water) and solute molecules. The experiments described in this paper and their analysis show how to reveal this contribution and give an estimation of its expected relevance.

Disclosure statement

No potential conflict of interest was reported by the authors.

Funding

This project has received funding from the European Union's Horizon 2020 Research and Innovation Programme under grant agreement No 665172.

ORCID

Danuta Kruk http://orcid.org/0000-0003-3083-9395

References

[1] R. Kimmich and E. Anoardo, Prog. Nucl. Magn. Reson. Spectrosc. **44**, 257 (2004).
[2] F. Fujara, D. Kruk and A.F. Privalov, Prog. Nucl. Magn. Reson. Spectrosc. **82**, 39 (2014).
[3] F. Winter and R. Kimmich, Mol. Phys. **45**, 33 (1982).
[4] F. Winter and R. Kimmich, Biophys. J. **48**, 331 (1985).
[5] E. Anoardo and D.J. Pusiol, Phys. Rev. Lett. **76**, 3983 (1996).
[6] I. Bertini, J. Kowalewski, C. Luchinat, T. Nilsson and G. Parigi, J. Chem. Phys. **111**, 5795 (1999).
[7] É. Tóth, L. Helm and A. E. Merbach, in Contrast Agents I, edited by W. Krause (Springer, Berlin, 2002), p. 61.
[8] P.-O. Westlund, Mol. Phys. **107**, 2141 (2009).
[9] P.-O. Westlund, Phys. Chem. Chem. Phys. **12**, 3136 (2010).
[10] D. Kruk, A. Kubica, W. Masierak, A.F. Privalov, M. Wojciechowski and W. Medycki, Solid State Nucl. Magn. Reson. **40**, 114 (2011).
[11] L.M. Broche, G.P. Ashcroft and D.J. Lurie, Magn. Reson. Med. **68**, 358 (2012).
[12] M. Florek-Wojciechowska, M. Wojciechowski, R. Jakubas, S.Z. Brym and D. Kruk, J. Chem. Phys. **144**, 054501 (2016).
[13] M. Florek-Wojciechowska, R. Jakubas and D. Kruk, Phys. Chem. Chem. Phys. **19**, 11197 (2017).
[14] I. Bertini, C. Luchinat and G. Parigi, Solution NMR of Paramagnetic Molecules (Elsevier, Amsterdam, 2001).
[15] D. Kruk and J. Kowalewski, Mol. Phys. **101**, 2861 (2003).
[16] J. Kowalewski, D. Kruk and G. Parigi, Adv. Inorg. Chem. **57**, 41 (2005).
[17] P. Caravan, Chem. Soc. Rev. **35**, 512 (2006).
[18] E. Belorizky, P.H. Fries, L. Helm, J. Kowalewski, D. Kruk and P.O. Westlund, J. Chem. Phys. **128**, 052315 (2008).
[19] D.J. Lurie, G.R. Davies, M.A. Foster and J.M. Hutchison, Magn. Reson. Imaging. **23**, 175 (2005).
[20] D.J. Lurie, Proc. Intl. Soc. Mag. Reson. Med. **292**, 1998 (1998).
[21] D.J. Lurie, S. Aime, S. Baroni, N.A. Booth, L.M. Broche, C.H. Choi, G.R. Davies, S. Ismail, DÓ hÓgáin and K.J. Pine, Comptes Rendus Phys. **11**, 136 (2010).
[22] S. Merbach, L. Helm, É Tóth, The Chemistry of Contrast Agents in Medical Magnetic Resonance Imaging (Wiley & Sons Ltd., Chichester, 2013).
[23] I. Solomon and N. Bloemebergen, J. Chem. Phys. **25**, 261 (1956).
[24] A. Abragam, The Principles of Nuclear Magnetism (Oxford University Press, Oxford, 1961).
[25] N. Bloembergen and L.O. Morgan, J. Chem. Phys. **34**, 842 (1961).
[26] C. Slichter, Principles of Magnetic Resonance (Springer-Verlag, Berlin, 1990).
[27] A. Redfield, in Encyclopedia of Nuclear Magnetic Resonance, edited by D. Grant and R. Harris (Wiley & Sons. Ltd., Chichester, 1996). pp. 4085–4092.
[28] J. Kowalewski and L. Mäler, Nuclear Spin Relaxation in Liquids: Theory, Experiments, and Applications (Taylor & Francis, New York, 2006).
[29] D. Kruk, Theory of Evolution and Relaxation of Multi-Spin Systems. Application to Nuclear Magnetic Resonance (NMR) and Electron Spin Resonance (ESR) (Abramis Academic, Arima Publishing, Suffolk, 2007).
[30] R. Meier, D. Kruk and E.A. Rössler, J. Chem. Phys. **136**, 34508 (2012).
[31] D. Kruk, Understanding Spin Dynamics (Pan Stanford Publishing Pte Ltd, Singapore, 2015).
[32] L.P. Hwang and J.H. Freed, J. Chem. Phys. **63**, 4017 (1975).
[33] D. Kruk, T. Nilsson and J. Kowalewski, Mol. Phys. **99**, 1435 (2001).
[34] D. Kruk, R. Meier and E.A. Rössler, J. Phys. Chem. B. **115**, 951 (2011).
[35] R. Meier, D. Kruk, J. Gmeiner and E.A. Rössler, J. Chem. Phys. **136**, 034508 (2012).